Mol. Cryst. Liq. Cryst., Vol. 617: pp. 109–118, 2015

ISSN: 1542-1406 print/1563-5287 online
DOI: 10.1080/15421406.2015.1075840

Influences of MgO Thicknesses Variation on Degradation Characteristics during Long-term Discharge in Microdischarge Cells

JAE HYUN KIM,[1] CHOON-SANG PARK,[2]
EUN-YOUNG JUNG,[3] SUNG-O KIM,[4]
AND HEUNG-SIK TAE[2,*]

[1]Radiation Instrumentation Research Division, Korea Atomic Energy Research Institute, Daejeon, Korea
[2]School of Electronics Engineering, College of IT Engineering, Kyungpook National University, Daegu, Korea
[3]Core Technology Lab., Corporate R&D Center, Samsung SDI Co. Ltd., Cheonan, Chungcheongnam-Do, Korea
[4]Department of Electrical and Computer Engineering, New York Institute of Technology, Old Westbury, NY, USA

This paper investigates the changes in the surface and discharge characteristics during long-term (1000-hour) discharge in microdischarge cells with MgO crystal powders as a parameter of the MgO thickness variation. For four different MgO thicknesses (2500, 3500, 4500, and 5500 Å), the changes in the MgO surfaces were monitored by the SEM, and X-ray diffraction (XRD), and the resultant changes in the discharge characteristics such as the firing voltage and address delay time were also examined during the long-term (1000-hour) discharge. When increasing the MgO thickness ranging from 2500 to 5500 Å, it was observed that the grain size increased and (111) peak was intensified. Also, after 1000-hour discharge, it was observed that the firing voltage increased slightly with an increase in the MgO thickness, whereas the address discharge delay decreased with an increase in the MgO thickness.

Keywords MgO layer; discharge characteristics; plasma application; plasma display panel

1. Introduction

The MgO layer in ac-plasma display panels plays an important role in producing the sustain and address discharge by lowering the firing voltage thanks to its high secondary electron emission coefficient [1, 2]. However, in the microdischarge cells of plasma display devices such as ac-plasma display panels, the MgO layer is exposed to a discharge space with

*Address correspondence to Prof. Heung-Sik Tae, School of Electronics Engineering, College of IT Engineering, Kyungpook National University, Sangyuk-dong, Buk-gu, Daegu 702-701, Korea. E-mail: hstae@ee.knu.ac.kr

Color versions of one or more of the figures in the article can be found online at www.tandfonline.com/gmcl.

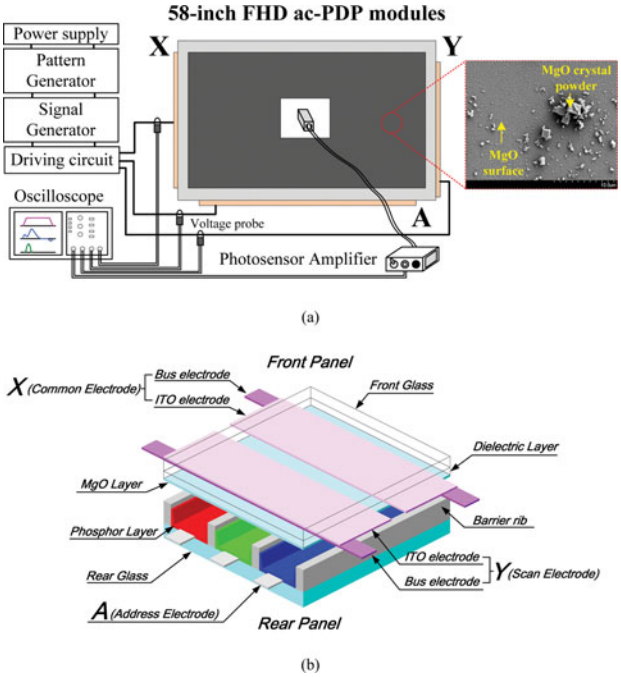

Figure 1. Schematic diagrams of experimental setup.

a ternary gas mixture of He-Ne-Xe. Consequently, the ions produced during discharge bombard severely the MgO surface, thereby resulting in deteriorating the function of MgO layer. Moreover, the damaged MgO layers in microdischarge PDP cells may induce an image sticking problem because the discharge characteristics can vary considerably depending on whether the MgO layers are damaged or not [3]. Recently, in order to improve the address delay characteristics and obtain the lower firing voltage, various types of MgO crystal powders have been additionally coated on the MgO layer as a functional layer for compensating the conventional MgO layer [4]. Meanwhile, the effects of the thickness of the MgO layer on the MgO film properties, such as crystal orientation, stoichiometry, film density, surface morphology, and roughness have been fully studied so far [5–8]. However, the correlation between the MgO thickness and its discharge degradation characteristics has been rarely reported. In particular, in the case of the MgO layer coated by the MgO crystal powders, the changes in the degradation characteristics including the discharge characteristics relative to the MgO thickness during a long time (>500 hours) discharges have not yet been studied in detail.

Accordingly, this paper investigates the influences of the thickness variation of MgO layer with MgO crystal powder on both degradation of MgO layer and corresponding discharge characteristics in the 58-in. full-HD AC-PDP test module with a He (35%)-Xe (11%)-Ne contents and box-type barrier. The variations in the firing voltage and address delay time were examined as functions of both the MgO thickness and discharge time in the case of the MgO layer coated by the MgO crystal powders. Furthermore, the changes in the MgO surface morphology including MgO crystal powders were also investigated.

Table 1. Specifications of 58-in. full-HD test panel in this study

Front panel		Rear panel	
ITO width	200 μm	Barrier rib width	60 μm
ITO gap	70 μm	Barrier rib height	120 μm
Bus width	90 μm	Address width	90 μm
Cell pitch		223 μm X 669 μm	
Gas pressure		420 Torr	
Gas chemistry		Ne-He(35%)-Xe(11%)	

2. Experimental Methods

Figure 1 (a) shows the optical measurement systems and 58-in. full-HD ac-PDP test modules with three electrodes, where X is the common electrode, Y is the scan electrode, and A is the address electrode. A pattern generator, a waveform generator, and a photosensor amplifier (Hamamatsu C6386) were used to measure the infrared (IR) emission and firing voltage. The 58-in. full-HD ac-PDP test modules employed in this study had the gas mixture of Ne-He (35%)-Xe (11%) and pressure of 420 Torr. Fig. 1 (b) shows a single pixel comprising the R, G, and B mocrodischarge cells employed in this study. The PDP cell conditions for the full-HD grade 58-inch ac-PDP test modules were all exactly the same, except for the MgO thickness variation. The detail panel specifications are listed in Table 1.

The MgO thin films were deposited on the dielectric layer of the ac-PDP by using the ion-plating evaporation [9], and the oxygen and hydrogen flow rates were kept at 200 and 120 sccm during deposition, respectively. The MgO crystal powders were coated on the MgO thin film by using the spray method. As shown in the scanning electron microscope (SEM) image of Fig. 1, the shape of MgO crystal powders was cubic, and their sizes ranged from a few tens of nanometers to a few micrometers. In this experiment, the MgO thin films with four different thicknesses (case1: 2500 Å, case 2: 3500Å, case 3: 4500 Å, and case 4: 5500Å, as shown in Table 2) were prepared to investigate the degradation characteristics of the MgO surface including the MgO crystal powders and the corresponding discharge characteristics relative to the thickness variation of the MgO layer during a long time (1000-hour) discharge. Figure 2 shows the conventional driving waveform, including the reset-, address-, and sustain–periods employed in this study. The sustain voltage and frequency during a sustain-period were 205 V and 200 kHz, respectively. The duty ratio of the sustain pulses was 40% and the total display time was 1000 hours. It is well-known that the degradation characteristics of MgO thin film are closely related to the severe ion bombardment during discharge [10, 11]. In addition, the SEM and XRD were used to inspect the changes in the surface morphology and crystallization of MgO thin films as a result of thickness variation under a severe long time bombardment condition.

Table 2. Thicknesses variations of MgO thin film in this study

	Case 1	Case 2	Case 3	Case 4
Thickness of MgO thin film	2500 Å	3500 Å	4500 Å	5500 Å

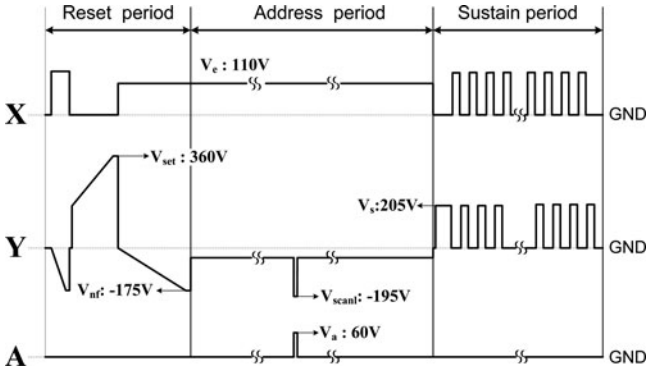

Figure 2. Schematic diagram of driving waveform employed to measure discharge characteristics.

Furthermore, the firing voltage between the X-Y electrodes and the address discharge delay time were measured to investigate the changes in the electron emission characteristics of the MgO surface as a result of thickness variation under a severe long time bombardment condition.

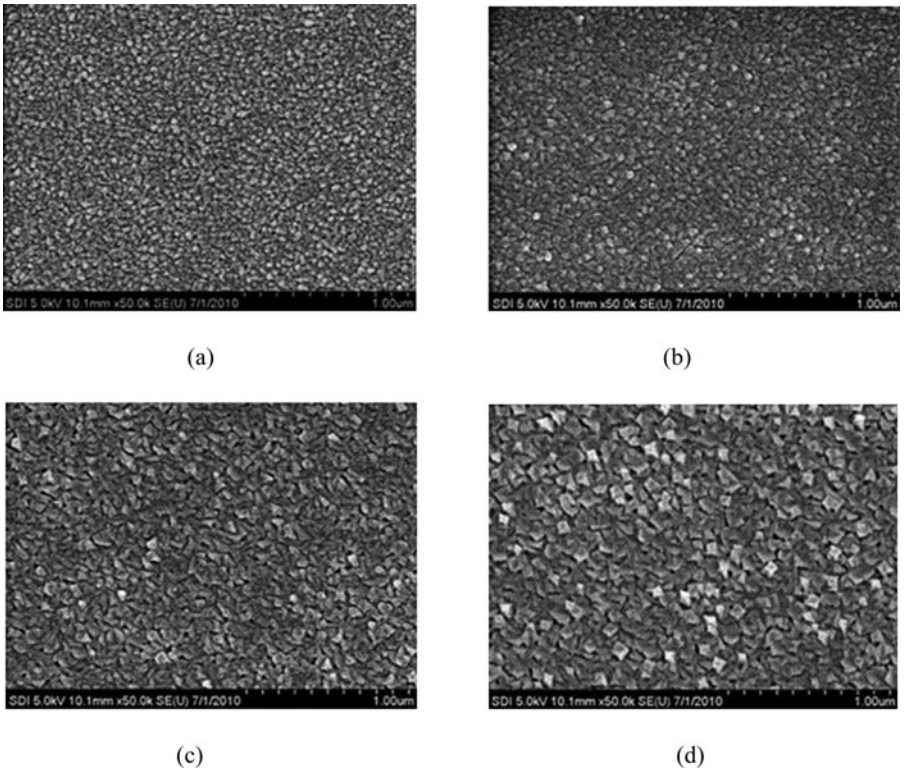

Figure 3. Comparison of plane-SEM image of MgO surface measured from 58-inch full-HD panels using MgO thin film with various thickness conditions: (a) case 1 (2500 Å), (b) case 2 (3500 Å), (c) case 3 (4500 Å), and (d) case 4 (5500 Å).

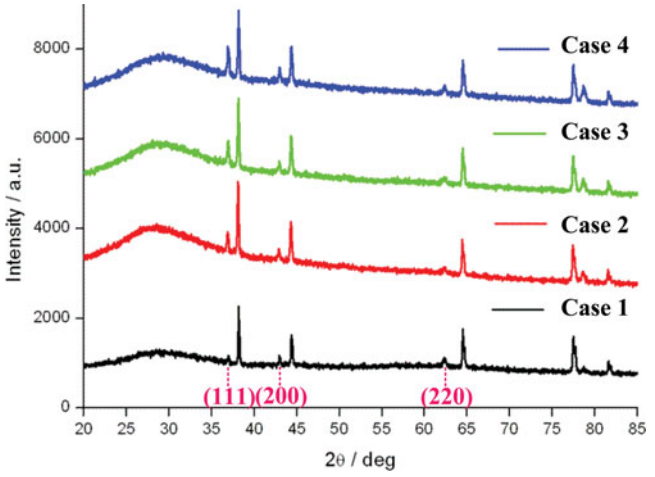

Figure 4. Dependence of X-ray diffraction patterns of MgO thin films with various thicknesses.

3. Results and Discussion

3.1. Surface and Discharge Characteristics of MgO Thin Film with MgO Crystal Powders Relative to MgO Thickness Variation at Initial Discharge State

Figure 3 shows the SEM images of the MgO surfaces with four different MgO thicknesses of the 58-in. FHD test panels employed in this research, where (a) is case 1: 2500Å, (b) is case 2: 3500 Å, (c) is case 3: 4500 Å, and (d) is case 4: 5500 Å. As shown in Fig. 3, with an increase in the MgO thickness, the grain size of the MgO surface was observed to be increased.

Figure 4 shows the X-ray diffraction (XRD) spectra of the MgO thin films with four different thicknesses of Fig. 3 measured by the X-ray Diffractometer (Panalytical X' pert Pro) with a Cu Kα X-ray source (wavelength of 1.54 Å) working at 40 kV and 40 mA. The XRD spectra of Fig. 4 was measured in $\theta/2\theta$ scans with a step size of 0.013° over the range of 2θ from 20° to 80°. The XRD spectra of Fig. 4 show the similar diffraction patterns having the (111), (200) and (220) peaks for all cases of Fig. 3. However, with an increase in the MgO thickness, the intensity of (111) peak was observed to be considerably increased. These (111) peaks of MgO surfaces were closely related to the secondary electron emission of the MgO surface [12, 13]. Accordingly, with an increase in the (111) peak, the firing voltage was reduced due to the increasing secondary electron emission [12, 13].

Figure 5 (a) shows the firing voltage between the X-Y electrodes relative to MgO thickness variation at initial discharge state. The firing voltage between X-Y electrodes showed such a tendency that the firing voltage between MgO surfaces decreased as increasing the MgO thickness. As described previously, the reduction of the firing voltage in Fig. 5 (a) as increasing the MgO thickness is due to the improvement of the secondary electron emission induced by intensifying the (111) peak of the MgO surface depending on the MgO thickness.

It is reported that the MgO crystal powder can contribute to enhancing the address discharge delay, especially statistical delay [4]. Thus, the address discharge delays for the MgO surface with MgO crystal powders in Fig. 5(b) show more improved delay characteristics than those for the MgO surface without MgO crystal powders. In addition,

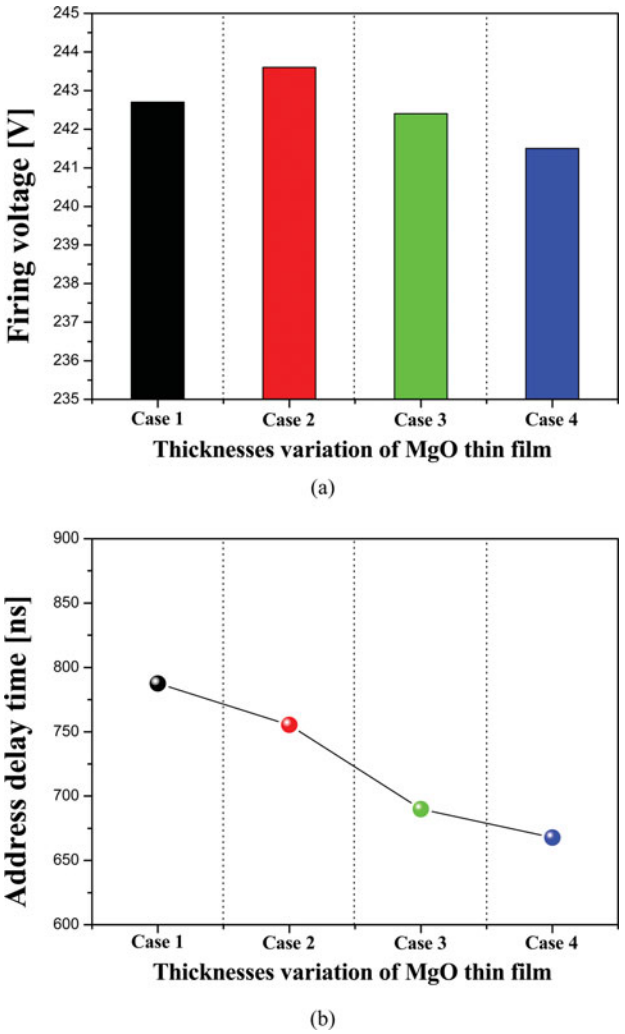

Figure 5. Comparison of discharge characteristics of MgO thin film with MgO crystal powders relative to MgO thickness before long-time discharge: (a) firing voltage between X-Y electrodes and (b) address delay time.

the formative delay as well as statistical delay can influence the address discharge delay characteristics, such that the secondary electron emission capability of MgO surface can also affect the address discharge characteristics. Consequently, since the secondary electron emission capability is improved with an increase in the MgO thickness, the resultant address delay time was observed to be decreased as increasing the MgO thickness, as shown in Fig. 5 (b).

3.2. Changes in Surface and Discharge Characteristics of MgO Thin Film with MgO Crystal Powders Relative to MgO Thickness Variation After Long-Term Discharge

Despite a low sputtering yield of the MgO thin film, variations of the MgO surface would seem to be unavoidable due to severe iterant ion bombardment, especially in the case

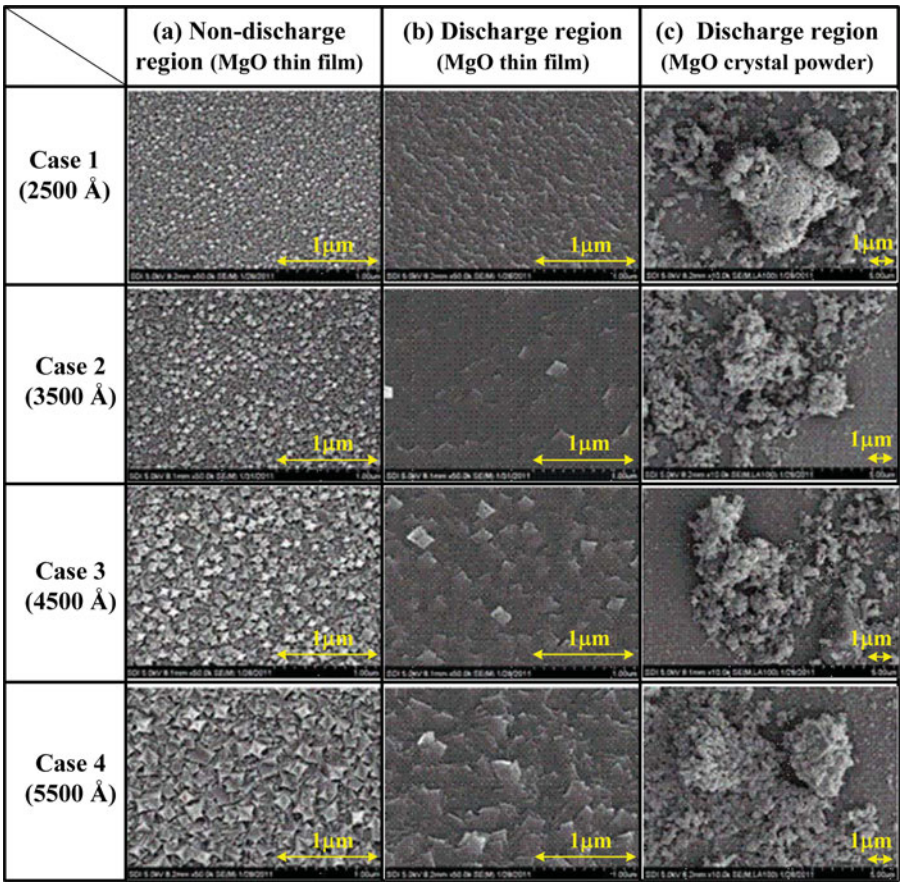

Figure 6. Comparison of SEM images of MgO surfaces according to MgO thickness after long-term (1000-hour) discharge: (a) non-discharge region, (b) discharge region and (c) discharge region MgO crystal powders.

of long-term discharge. Thus, the discharge characteristics depending on the MgO surface would be degraded due to the deterioration of the MgO surface exposed to the severe ion bombardment during a long period. In particular, the changes in the MgO surface morphology induced by the severe iterant ion bombardment can significantly influence the second electron emission characteristics [15]. In this experiment, the changes in the morphology of the MgO surface including the MgO crystal powders and the corresponding discharge characteristics such as firing voltage and address delay time were investigated after a long-term (1000 hours) discharge as a function of the MgO thickness variation.

Figure 6 shows the SEM images of the MgO surfaces with four different MgO thicknesses measured after the 1000-hour discharge for the three different regions, *i.e.*, (a) MgO surface in non-discharge region, (b) MgO surface in discharge region, and (c) MgO crystal powders in discharge region. After 1000-hour discharge, the grains with pyramidal morphologies still remained irrespective of MgO thickness variation, as shown in Fig. 6 (a). Whereas, these pyramidal morphologies were observed to be destroyed in the MgO surfaces in the discharge region, and the destruction of MgO surface morphologies were observed to be severe with an increase in the MgO thickness, as shown Fig. 6 (b) and

Table 3. Changes in sputtered thickness of MgO thin film with four different MgO thicknesses measured by Eillpsometer

	Non-discharge region	Discharge region	Sputtered thickness
Case 1 (2500 Å)	2505 Å	2240 Å	265 Å
Case 2 (3500 Å)	3571 Å	3108 Å	463 Å
Case 3 (4500 Å)	4439 Å	3844 Å	595 Å
Case 4 (5500 Å)	6548 Å	5890 Å	658 Å

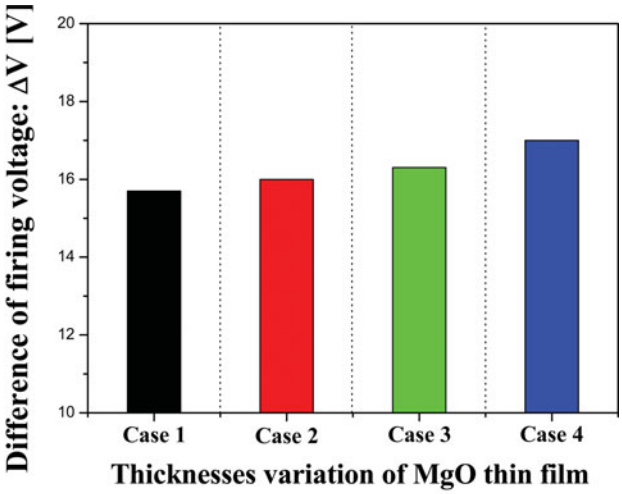

(a)

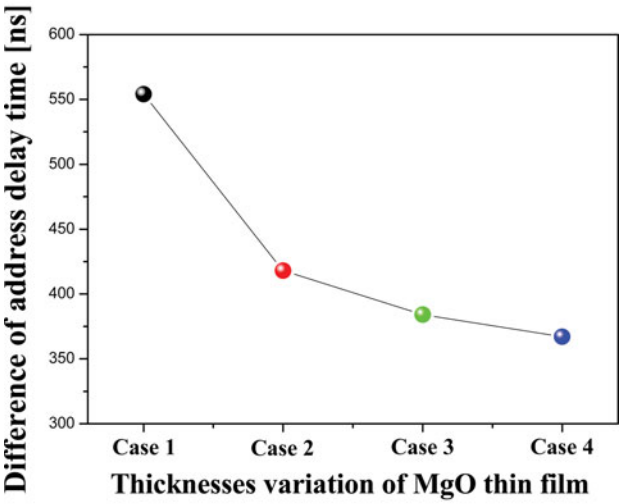

(b)

Figure 7. Differences in (a) firing voltage and (b) address delay time before and after long-time (1000-hour) discharge relative to MgO thickness.

Table 3. This experimental result indicates that as the MgO thickness is increased, the MgO surface experience severe ion damage presumably due to the increase in the ion density induced by the improvement of secondary electron emission deeply related to the MgO thickness variation. On the other hand, as shown in all cases of Fig. 6 (c), parts of MgO crystal powders were founded to still remain on the MgO surface after 1000-hour discharge, even though all the MgO crystal powders could not survive on the MgO surface during severe iterant ion bombardment. As shown in Fig. 6 (c), the MgO crystal powder could be protected from the severe iterant ion bombardment thanks to the re-deposition of the Mg particles sputtered from the MgO surface.

Figures 7 (a) and (b) show the differences of firing voltage and address delay time between the initial state and after 1000-hour discharge for all cases, *i.e*., four different MgO thicknesses. As shown in Figs. 7 (a) and (b), with an increase in the MgO thickness, the change in the firing voltage between the X-Y electrodes was observed to slightly increase, while the changes in the address delay time decreased as increasing the MgO thickness. The result of Fig. 7 (a) implies that in the case of low firing voltage, for example, the lowest firing voltage in case 4, the MgO surface quality for producing a discharge is more aggravated during severe iterant ion bombardment, *i.e*., the highest firing voltage in case 4 after 1000-hour discharge. On the other hand, as the MgO surface is more sputtered due to the increase in the ion density induced by the improvement of secondary electron emission, it would be possible to protect the MgO crystal powders effectively by means of the re-deposition of the sputtered Mg particles in to the MgO crystal powders. Accordingly, the changes in the address delay time of Fig. 7 (b) are related to the amount of the MgO crystal powders remaining during severe iterant ion bombardment, meaning that the degradation characteristics of address discharge delay after 1000-hour discharge strongly depend on the preservation of the MgO crystal powders.

Conclusion

We investigate the changes in the degradation characteristics of MgO thin film with MgO crystal powders in case of adopting four different MgO thicknesses. Our experimental results show that in the case of MgO thin film coated by MgO crystal powders, the secondary electron emissions can be improved by adjusting the MgO thickness and furthermore the degradation discharge characteristics including both firing voltage and address discharge delay strongly depend on the MgO thickness. It is expected that these experimental results will help to enhance the life-time or to solve the image quality problem in the PDP-TVs.

Funding

This research was supported by Basic Science Research Program through the National Research Foundation of Korea (NRF) funded by the Ministry of Education (2013R1A1A4A03008577).

References

[1] Boeuf, J. P. (2003). *J. Phys. D: Appl. Phys.*, *36*, R53.
[2] Ha, C. H., Kim, J. K., & Whang, K.-W. (2007). *J. Appl. Phys.*, *101*, 123301.
[3] Park, C.-S., Tae, H.-S., & Chien, S.-I. (2011). *Appl. Phys. Lett.*, *99*, 083503[1].
[4] Kim, J. H., Park, C.-S., Park, H. D., Tae, H.-S., & Lee, S.-H. (2012). *J. Nanosci. Nanotechnol.*, *13*, 3270.

[5] Fujiia, E., Tomozawaa, A., Toriia, H., & Nagakib, T. (1999). *Thin. Solid. Films. 352*, 85.
[6] Son, C. Y., Cho, J. H., & Park, J.-W. (1999). *J. Vac. Sci. Technol. A*, *17*, 2619.
[7] Pan, C., O'Keefe, P., & Kester, J. J. (1998). *in Proc. SID'98 Dig.* p. 865.
[8] Park, S. Y., Lee, M. J., Kim, H. J., Moon, S. H., Kim, S. G., & Kim, J. K. (2005). *J. Vac. Sci. Technol. A*, *23*, 1162.
[9] Oumi, K., Matsumoto, H., Kashiwagi, K., & Murayama, Y. (2003). *Surf. Coat. Technol.*, *562*, 169.
[10] Yu, Z.-N., Seo, J.-W., Zheng, D.-X., & Sun, J. A. (2003). *Surf. Coat. Technol.*, *398*, 163.
[11] Park, C.-S. & Tae, H.-S. (2010). *Appl. Phys. Lett.*, *96*, 043504.
[12] Jeong, J.-Y., Cho, S.-Y., Lee, D.-K., Lee, H.-J., Lee, H.-J., & Park, C.-H. (2009). *Trans KIEE*, *58*, 1566.
[13] Choi, E.-H. (1998). *Jpn. J. Appl. Phys.*, *37*, 7015.
[14] Park, C.-S., Tae, H.-S., Jung, E.-Y., Seo, J. H., & Shin, B. J. (2010). *IEEE Trans. Plasma Sci.*, *38*, 2439.